COUPLED CFD-MPM FOR MODELLING DEBRIS FLOW UNDER THE WATER

QUOC-ANH TRAN*, GUSTAV GRIMSTAD, SEYED ALI GHOREISHIAN AMIRI

Department of Civil and Environmental Engineering

Norwegian University of Science and Technology

Trondheim, Norway

* tran.quocanh@aalto.fi

Key words: Material Point Method, Computational Fluid Dynamics, multi-phase flow, submarine landslides.

Abstract. Simulating the submarine debris flows is challenging as it involves a complex interaction between debris flow (solid) and seawater (fluid). However, debris flow simulation in literature relied on only either particle-based method or Computational Fluid Dynamics (CFD). This paper presents a different approach to simulate the solid-fluid interaction (e.g. submarine landslides). The presented model couples the CFD with the Material Point Method (MPM). In brief, the CFD handles the flow dynamics of the seawater while the MPM captures the mechanism of debris flow in the framework of solid mechanics. A numerical simulation is performed and compared with experimental results to highlight the capability of the coupled CFD-MPM model. Such a model can support engineers to have better understanding of the mechanism of submarine debris flows and possible impacts on offshore infrastructure.

1.   INTRODUCTION

Submarine landslides can pose significant threats to the offshore infrastructures and the coastal communities. To evaluate the risk of the submarine slides, it is necessary to model their dynamics which involve a complex solid-fluid interaction between submarine debris flow and seawater. Numerical methods to simulate the submarine landslides can be classified into Computational Fluid Dynamics (CFD) methods and particle-based methods. To simulate the submarine slides, CFD methods solve governing equations in a full-Eulerian framework for single-phase flows [1, 2] and for multi-phase flows [3, 4] with interface capturing techniques to track material interfaces. Although complex flows can be captured in CFD (such as turbulent flows), CFD cannot efficiently consider the 'true non-linear soil constitutive laws' because tracking the spatial/time-dependent state variables of debris materials in the Eulerian framework is not straightforward. Consequently, some initiation mechanisms of submarine landslides cannot be explained with only simple constitutive models. On the other hand, particle-based methods can overcome this problem by adopting the Lagrangian framework for solid materials. This class of methods has been extensively used to simulate submarine landslides such as Material Point Method (MPM) [5], Smooth Particle Hydro Dynamics [6], Particle Finite Element Method [7], or Coupled Eulerian Lagrangian method [8]. But these simulations neglected the complex fluid flows of seawater interacting with the submarine debris flow for simplicity. Even if fluid flows are considered, particle-based methods have numerical pressure instability in modelling the fluid flow which requires additional numerical treatments such as B-bar method [9], null-space filter [10], or least square approximation [11, 12, 13]. Indeed, CFD is a more optimal option for complex fluid flows especially dealing with large distortions of

continuum fluid media.

Therefore, it could be ideal to couple CFD with particle-based methods to take advantages of both approaches. Although the last two decades have witnessed significant development of particle-based methods to solve large deformation of solids with more than 50 methods up to date [14], the MPM appears as one of the best candidates to couple with CFD. This is because MPM incorporates a stationary mesh during the computation in a similar way to the CFD. As such, both MPM and CFD can be coupled naturally in a unified computational mesh. This paper presents a description of a coupled CFD-MPM method to simulate the debris flow under the water. We perform a numerical analysis by comparing with the experimental results from the experiment conducted by Rzadkiewicz and co-workers [15]. This preliminary result demonstrates the capability of the CFD-MPM model. More realistic constitutive laws, and governing equations of multi-phase flows will be implemented in the future. Instructions for replicating the numerical result in this paper are given at the open-source platform GitHub [16]. Also, the open-source code is shared in this platform for interest users to take up and make use of the results.

2. NUMERICAL MODELING APPROACH

Modeling Approach

In this paper, we present a coupled CFD-MPM method where MPM handles the large deformation of the solid materials while CFD performs the fluid dynamics analysis. For example, in the modelling of the debris flow under water (Figure 1), MPM is used to model the seabed and the debris flows while CFD is used to model the fluid dynamics (water and air) using Navier-Stokes. By coupling CFD with MPM, the presented method can preserve the advantages of both CFD and MPM. Indeed, MPM allows to define more complex solid/soil constitutive models which are crucial for the initiation mechanism of the flow. The solids (MPM materials) are interacted through the contact laws, such as Coulomb's friction. On the other hand, CFD is the conventional method to simulate the complex viscous fluid flows involving turbulence (flow undergoes irregular fluctuations) or hydroplaning (debris flows lose frictional resistance with the seabed). Overall, the coupled CFD-MPM method can capture complex mechanisms involving solid-fluid interaction in the simulations of debris flow under water.
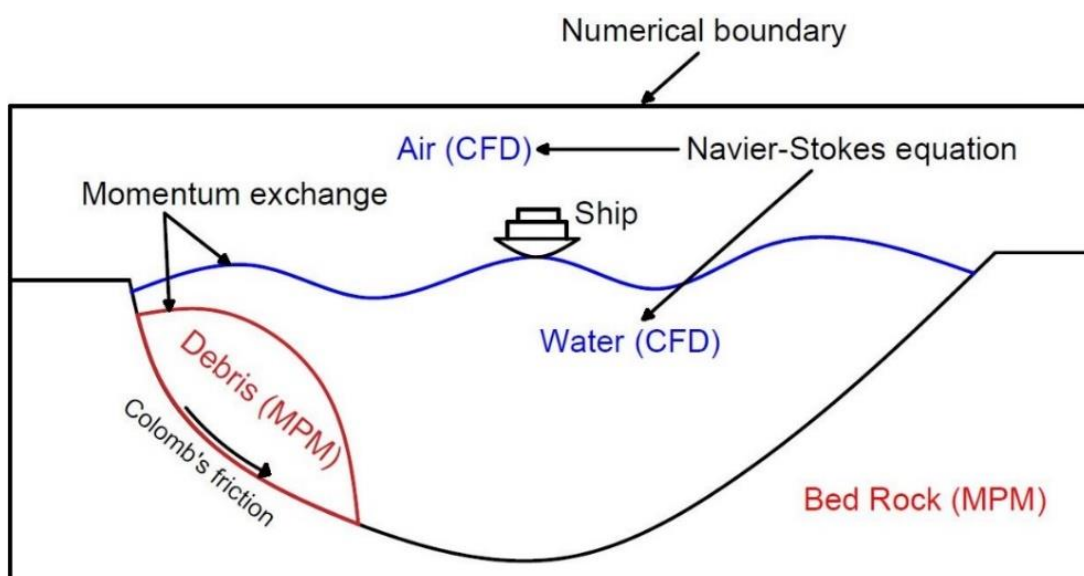

Figure 1. *Schematic of coupled CFD-MPM model*

Brief description of the coupled CFD-MPM model

The coupled CFD-MPM model was developed and implemented in the Uintah computational framework [17]. It has been used for sophisticated fluid-structure interaction such as simulations of deflagration [18] or spinal cord injury [19]. However, simulation of debris flows is unexplored up to date. The multi-material CFD approach is derived from the implicit continuous-fluid Eulerian method (ICE). The development of ICE method can be found in Kashiwa (2001) [20]. In ICE, all state variables are located at the cell/body centers (in contrast to a staggered grid in which the velocity is located at faced centers). In an arbitrary volume, the average state variables at cell centers are given in the vector form of the material r $(M_r, \mathbf{u}_r, e_r, T_r, p, \theta_r, v_r)$ including mass, velocity, internal energy, temperature, pressure, volume fraction and specific volume. The following governing equations are solved at the Eulerian background mesh

Mass Balance Equation

$$\frac{1}{V}\frac{D_r M_r}{Dt} = 0 \tag{1}$$

Momentum Balance Equation

$$\frac{1}{V}\frac{D_r(M_r\mathbf{u}_r)}{Dt} = \nabla(\theta_r p) + \nabla\cdot(\theta_r\tau_r) + \rho_r\mathbf{g} + \sum\mathbf{f}_{rs} \tag{2}$$

In the right-hand side, the second term comes from the momentum change due to average shear stress τ_r and the turbulent effect can be considered in this term. The last term is the momentum exchange between materials $\mathbf{f}_{rs} = K_{rs}\theta_r\theta_s(\mathbf{u}_r - \mathbf{u}_s)$ with K_{rs} is the momentum exchange coefficient.

Energy Balance Equation

$$\frac{1}{V}\frac{D_r(M_r e_r)}{Dt} = -\rho_r p\frac{D_r v_r}{Dt} + \theta_r\tau_r : \nabla\mathbf{u}_r - \nabla\cdot\mathbf{j}_r + \sum q_{rs} \tag{3}$$

where the heat flux $\mathbf{j}_r = -\rho_r\beta_r\nabla T_r$, where β_r is the thermal diffusion coefficient, and the heat exchange $q_{rs} = H_{rs}\theta_r\theta_s(T_r - T_s)$, where H_{rs} is the heat exchange coefficient.

The MPM approach in this paper adopt the generalized interpolation technique from Bardenhagen and Kober [21]. This method was implemented in Uintah and validated with laboratory experiments [22, 23] and large-scale landslide [24]. To couple MPM with ICE, the state variables of MPM material points including $(M_p, \mathbf{u}_p, T_p, v_p)$ are mapped to cell centers using generalized interpolation technique. Then, both solid (MPM) and fluid (ICE) materials are solved using the set of multi-material governing equations (1), (2) and (3) using implicit integration scheme. This is also combined with the generalized Poisson's equation to compute the fluid pressure for compressible fluid materials.

Equation of state for fluid

Unlike solid materials, fluid mechanics adopts the equation of states to build the relations of the state variables pressure p, temperature T, and density $\rho = 1/v$. For example, it is possible to model the air using the equation of state for the perfect gas which obey the relationship

$$p = \rho RT \tag{4}$$

where R is the gas constant.

For the water, a simple linear equation of state is in the following form:

$$p - p_o = K_f\left[(\rho - \rho_o) - \beta(T - T_o)\right] \tag{5}$$

where reference pressure p_o = 1 atm = 101325 Pa, reference temperature T_o = 10°C, reference density ρ_o = 999.8 kg/m3, the bulk modulus of water K_f = 2.15e6 kPa, and the water thermal expansion β = 0.18 kg/m3 per Celsius degree.

Constitutive model for solid materials

In the paper, the basic undrained behavior of the soil is described by a simple elasto-plastic Tresca material model with no plastic volume change during shearing. The soil parameters include bulk modulus K, shear modulus G and yielding stress σ_y. The rigid bed is modeled by Neo-Hookean hyper elastic model with elasticity parameter including bulk modulus K, shear modulus G.

3. NUMERICAL EXAMPLE: DEBRIS FLOW UNDER WATER

The numerical example is validated with the experiment of submarine debris flow performed by Rzadkiewicz *et al.* [15]. In the experiment sand at rest in a triangular box is released and then the sand slides along the 45 degree-inclined rigid bed under water, see figure 2.
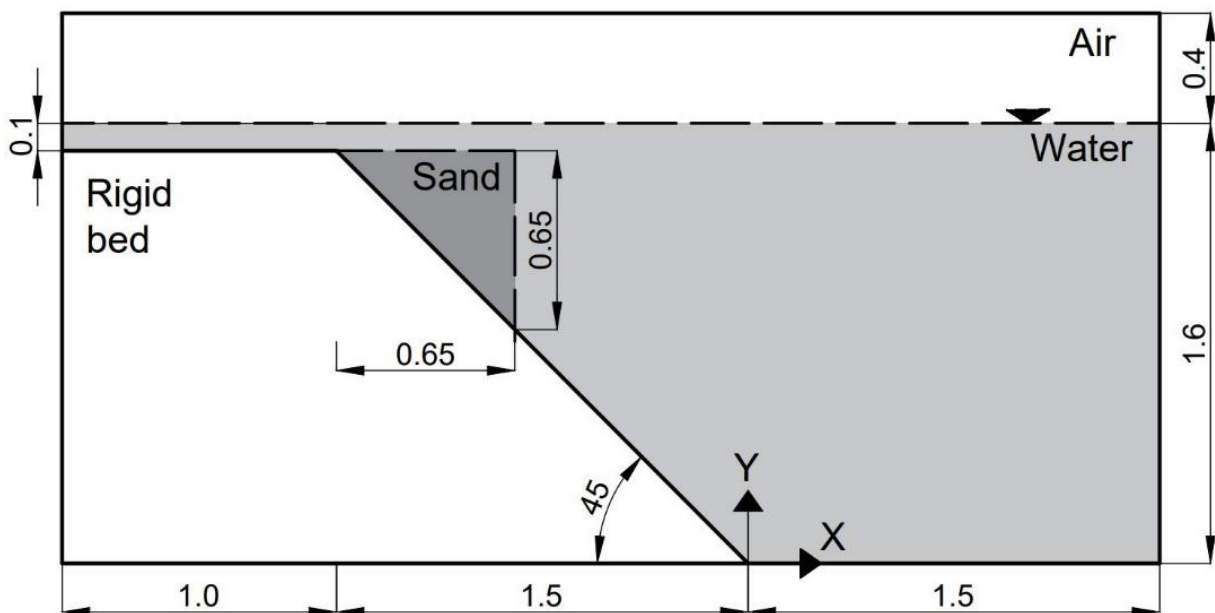

***Figure 2.*** *Schematic illustration of the experiment for under water debris flow*

In the numerical model, the material properties are selected as indicated in the experiment by Rzadkiewicz *et al.* [15]. The sand is modeled with the mean saturated density of 1985 kg/m3 and the yielding stress is 200Pa. Because the soil undergoes large deformation, the influence of the Young's modulus is negligible to the run-out mechanism of the debris flow. Therefore, we select the Young's modulus of 50MPa with the Poisson's ratio of 0.25. The rigid bed has much higher stiffness with the bulk modulus and shear modulus of 117.0e7 and 43.8e7. The water has the density of 999.8 kg/m3 and pressure of 1 atm at the water level surface which increases gradually with depth under gravity. The air has density of 1.17 kg/m^3 and atmospheric pressure of 1 atm on the top boundary. The viscosity of both air and water are 18.45e^{-6} and 855e^{-6} which corresponding to the temperature of air and water at 5°. Table 1 summarizes the numerical parameters used in this example.

Table 1. *Material parameters at the initial state*

Materials	Bulk modulus (Pa)	Shear modulus (Pa)	Density (kg/m³)	Temperature (Celsius)	Dynamic Viscosity (Pa s)	Yield Stress (Pa)
Water (at y = 1.6m)	2.15e⁶	-	999.8	5°	855e⁻⁶	-
Air (at y = 2.0m)	-	-	1.1768	5°	18.45e⁻⁶	-
Sand	8.33e⁶	20e⁶	1985	5°	-	200
Rigid bed	117.0e⁷	43.8e⁷	8900	5°	-	-

In all the boundary face, the Dirichlet boundary condition is imposed for velocity (u = 0m/s) and for the temperature (T = 5°) while the Neuman boundary condition is imposed for the pressure ($\frac{dp}{dx} = 0$ kPa) and density ($\frac{d\rho}{dx} = 0$ kg/m³). The size of the mesh is 5mm leading to 700 x 400 = 280.000 cells for the background mesh. The debris flow and rigid bed consist of a set of material points with the resolution of 2 x 2 material points in each cell.

Figure 3 and Figure 4 show the snapshots of the debris flow sliding in the plane at 0.4s and 0.8s. As shown, our simulated results have a good agreement with the computed results from Rzadkiewicz *et al.* [15] (see the red dots). Furthermore, typical mechanism of the debris flows under water are captured from the model (e.g. hydroplaning initiation in Figure 4 and the turbulent vortex in Figure 5). Figure 6 and Figure 7 show the comparison between our proposed method with experiment and other methods in terms of the elevation of the free surface at 0.4s and 0.8s. Again, our computed results replicated satisfactorily with the experiment and the computed results from Zhang *et al.* [7]. To replicate the numerical results for interested readers, the instructions and results are given at the open-source platform GitHub [16].
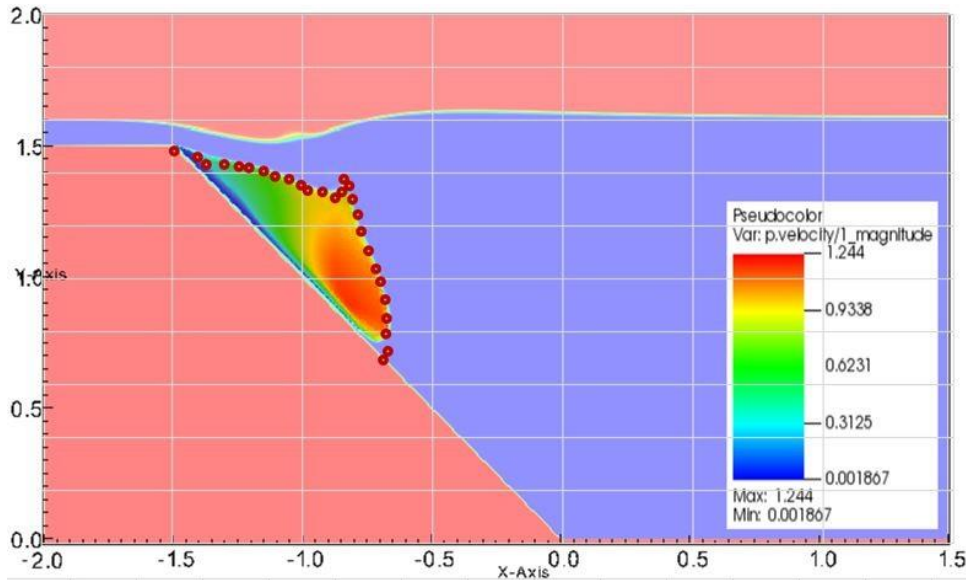
Figure 3. *Snapshot at 0.4s in the experiment, red dot is computed results [15]*
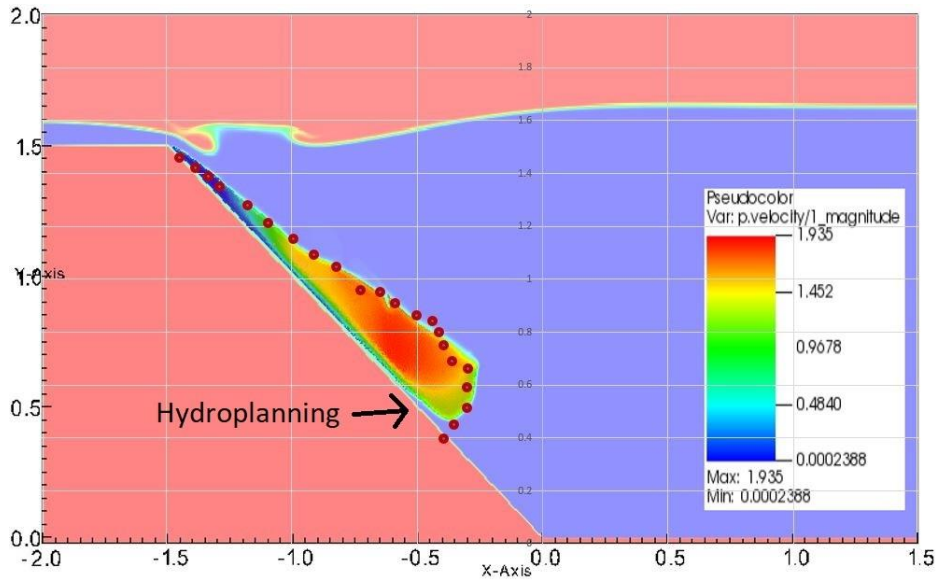
Figure 4. *Snapshot at 0.8s in the experiment, red dot is computed results [15]*
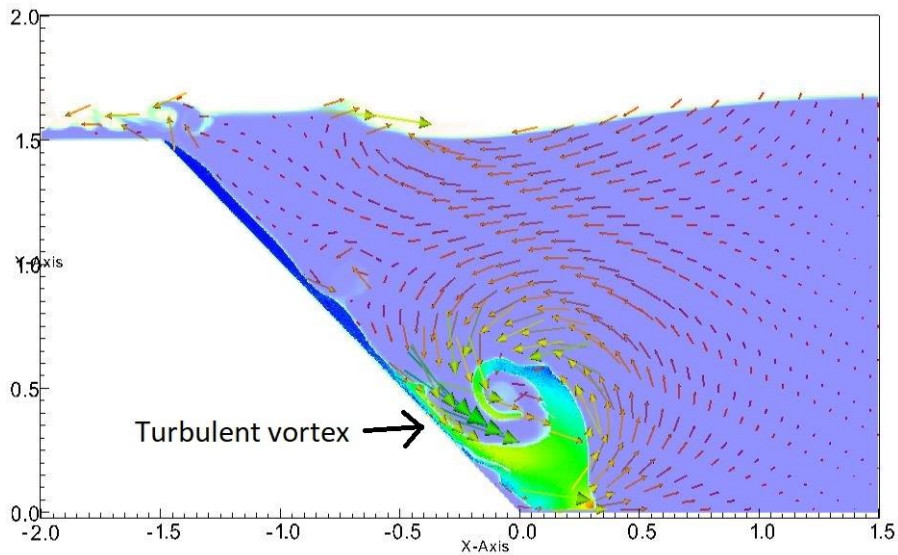

Figure 5. *Fluid velocity vector field in the soil-fluid interaction at 1.4s*
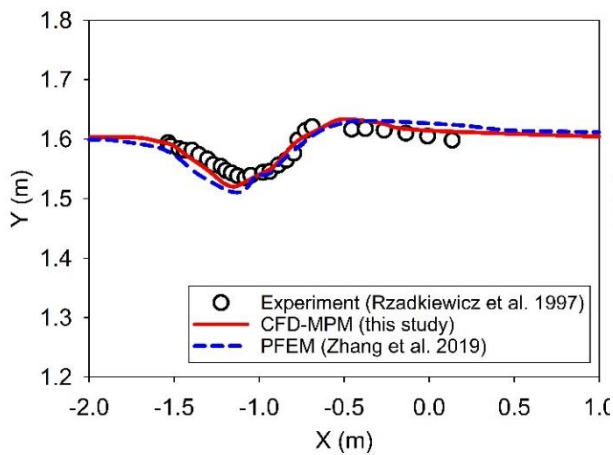

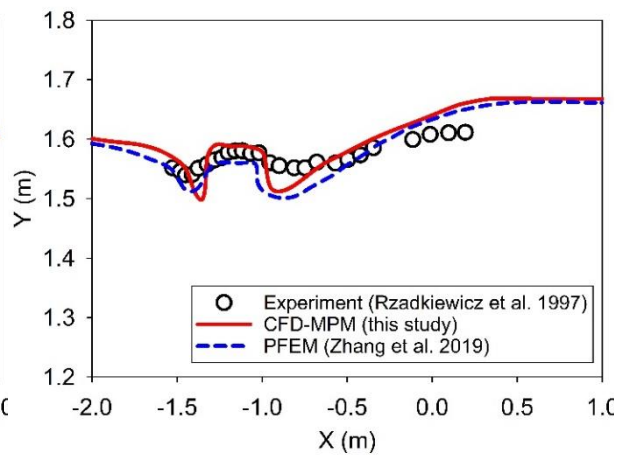**Figure 6.** *Elevation of the free surface at time of 0.4s*   **Figure 7.** *Elevation of the free surface at time of 0.8s*

4.   CONCLUSION AND OUTLOOK

This paper demonstrates preliminary results of the coupled CFD-MPM method to simulating the complex solid-fluid interaction in the hydro-mechanical-thermal coupling. In brief, CFD handles the complex viscous fluid flow while MPM solves the large deformation of the solid materials. Within the continuum mechanics framework, the tool allows to insert any material, fluid flow and thermal flow models. This brings enormous potential for many applications, not limited to submarine debris flow example presented here. Nevertheless, the numerical example demonstrated the capabilities as the typical mechanism of the underwater debris flows, the hydroplaning initiation and the turbulent vortex were captured in the simulation. The simulation result of matched well with the elevation of the free surface from the previous experimental result in time.

Further work

Although coupling of CFD-MPM is a promising tool for simulating complex solid-fluid interaction, there are still several limitations of the model.
-    The constitutive model for soil is rather simple and it has not yet considered the pressure-dependency.
-    There is mass exchange between soil and water when soil particle dissolves into the water at the interface. However, the coupled model has not yet considered this mass exchange.

These limitations will be addressed in the future research.

5.   ACKNOWLEDGEMENT

6.   REFERENCES

[1]   D. Yuk, S. C. Yim and P. L. Liu, "Numerical modeling of submarine mass-movement generated waves using RANS model," *Computers & Geosciences,* vol. 32, no. 7, pp. 927-935, 2006.

[2]   J. Kim, F. Løvholt, D. Issler and C. F. Forsberg, "Landslide Material Control on Tsunami Genesis—The Storegga Slide and Tsunami (8,100 Years BP)," *Journal of Geophysical Research: Oceans,* vol. 124, no. 6, pp. 3607-3627, 2019.

[3]   S. Abadie, D. Morichon, S. Grilli and S. Glockner, "Numerical simulation of waves generated by landslides using a multiple-fluid Navier–Stokes model," *Coastal Engineering,* vol. 57, no. 9, pp. 779-794, 2010.

[4]   P. Gauer, T. J. Kvalstad, C. F. Forsberg, P. Bryn and K. Berg, "The last phase of the Storegga Slide: simulation of retrogressive slide dynamics and comparison with slide-scar morphology," *Marine and Petroleum Geology,* vol. 22, no. 1-2, pp. 171-178, 2005.

[5]   J. J. Shi, W. Zhang, B. Wang, C. Y. Li and B. Pan, "Simulation of a Submarine Landslide Using the Coupled Material Point Method," *Mathematical Problems in Engineering,* pp. 1-14, 2020.

[6]   T. Capone, A. Panizzo and J. Monaghan, "SPH modelling of water waves generated by submarine landslides," *Journal ofHydraulic Research,* vol. 48, no. 1, pp. 80-84, 2010.

[7]   X. Zhang, E. Onate, S. A. G. Torres, J. Bleyer and K. Krabbenhoft, "A unified Lagrangian formulation for solid and fluid dynamics and its possibility for modelling submarine landslides and their consequences," *Computer methods in applied mechanics and engineering,* vol. 343, pp. 314-338, 2019.

[8]   R. Dey, C. Hawlader, R. Phillips and K. Soga, "Numerical modelling of submarine landslides with sensitive clay layers," *Géotechnique,* vol. 66, no. 6, pp. 454-468, 2016.

[9]   S. Bandara and K. Soga, "Coupling of soil deformation and pore fluid flow using material point method," *Computers and Geotechnics,* vol. 63, pp. 199-214, 2015.

[10]   Q. A. Tran and W. Sołowski, "Temporal and null-space filter for the material point method," *International Journal for Numerical Methods in Engineering,* vol. 120, no. 3, pp. 328-360, 2019.

[11]   X. Zheng, F. Pisano, P. Vardon and M. A. Hicks, "An explicit stabilised material point method for coupled hydromechanical problems in two-phase porous media," *Computers and Geotechnics,* vol. 135, p. 104112, 2021.

[12]   Q. A. Tran, E. D. Wobbes, W. Sołowski, M. Moller and C. Vuik, "Moving least squares reconstruction for B-spline Material Point Method," in *International Conference on the Material Point Method for Modelling Soil-Water-Structure Interaction*, Cambridge, UK, 2019.

[13]   Q. A. Tran, M. Berzins and W. Sołowski, "An improved moving least squares method for the Material Point Method," in *International Conference on the Material Point Method for Modelling Soil-Water-Structure Interaction*, Cambridge, UK, 2019.

[14]   J. S. Chen, M. Hillman and S. W. Chi, "Meshfree Methods: Progress Made after 20 Years," *Journal of Engineering Mechanics,* vol. 143, no. 4, p. 04017001, 2017.

[15]   S. A. Rzadkiewicz, C. Mariotti and P. Heinrich, "Numerical simulation of submarine landslides and their hydraulic effects," *Journal of Waterway, Port, Coastal, and Ocean Engineering,* vol. 123, no. 4, pp. 149-157, 1997.

[16]   "https://github.com/Uintah/Uintah/tree/master/src/StandAlone/inputs/MPMICE/SUBSLIDE/Sandbox," [Online].

[17]   J. E. Guilkey, T. Harman and B. Banerjee, "An Eulerian–Lagrangian approach for simulating explosions of energetic devices," *Computers & Structures,* vol. 85, no. 11-14, pp. 660-674, 2007.

[18]   J. Beckvermit, T. Harman, A. Bezdjian and C. Wight, "Modeling Deflagration in Energetic Materials using the Uintah Computational Framework," *Procedia Computer Science,* vol. 51, pp. 552-561, 2015.

[19]   S. T. Goode, "Development of a Spinal Cord Injury Model using the Material Point Method," PhD thesis, University of Leeds., 2016.

[20]   B. A. Kashiwa, "A multifield model and method for fluid–structure interaction dynamics," Technical Report LA-UR-01-1136, Los Alamos National Laboratory, Los Alamos, USA, 2001.

[21]   S. G. Bardenhagen and E. M. Kober, "The Generalized Interpolation Material Point Method," *Computer Modeling in Engineering & Sciences,* vol. 5, no. 6, pp. 477-496, 2004.

[22]   Q. A. Tran, W. Sołowski, M. Karstunen and L. Korkiala-Tanttu, "Modelling of Fall-cone tests with Strain-rate Effects," *Procedia Engineering,* vol. 175, pp. 293-301, 2017.

[23]   Q. A. Tran, W. Sołowski, V. Thakur and M. Karstunen, "Modelling of the Quickness test of Sensitive Clays using the Generalized Interpolation Material Point Method," in *Landslides in Sensitive Clays. Advances in Natural and Technological Hazards Research*, Springer, 2017, pp. 232-336.

[24]   Q. A. Tran and W. Sołowski, "Generalized Interpolation Material Point Method modelling of large deformation problems including strain-rate effects – Application to penetration and progressive failure problems," *Computers and Geotechnics,* vol. 106, pp. 249-265, 2019.